

CONTENTS – E through F

3D Tomographic Measurements on Allende Volumes — Constraints on the Formation and Accretion of Chondrules and Matrix <i>D. S. Ebel, T. W. Schoenbeck, and H. Palme</i>	5153
I-Xe Age of the Yamato 74191 (L3.6) Chondrite: Late Closure Time for I-Xe System with Enrichments in Halogens <i>N. Ebisawa, R. Okazaki, and K. Nagao</i>	5165
Calculation and Prediction of Hydrothermal Zones and Impact Conditions on Argyre Planitia, Mars <i>J. C. Echaurren and A. C. Ocampo</i>	5009
New Calculations and Estimations for Hydrothermal Zones and Impact Conditions on Chicxulub, Earth and Isidis Planitia, Mars <i>J. C. Echaurren and A. C. Ocampo</i>	5008
A Mathematic Model for the Araguinha Impact Structure, Brazil, South America <i>J. C. Echaurren, A. C. Ocampo, and M. C. L. Rocca</i>	5004
Water-Soluble Salts in Oman Desert Chondrites <i>D. Eggenschwiler, U. Krähenbühl, and B. Hofmann</i>	5045
A Super-Hard, Transparent Carbon Form, Diamond and Secondary Graphite in the Haverö Ureilite: A-Fine-Scale MicroRaman and Synchrotron Tomography <i>A. El Goresy, Ph. Gillet, L. Dubrovinsky, M. Chen, and T. Nakamura</i>	5061
The Chicxulub Impact: Results of Petrophysical and Paleomagnetic Investigations <i>T. Elbra, L. J. Pesonen, T. Kenkmann, and J. Smit</i>	5073
A 3D Investigation of Valles Marineris <i>B. E. Elliott and J. G. Spray</i>	5187
Trace Element Abundances in Chondrules from Knyahinya (L/LL5) and Ouzina (R4) <i>A. Engler, G. Kurat, and P. J. Sylvester</i>	5072
Evidence for a Two-Layer Structure of the Acapulcoite/Lodranite Parent Asteroid and 5 Ma CRE Age of 4 New Acapulcoites <i>O. Eugster and S. Lorenzetti</i>	5010
Deciphering Multiple Alteration Events in Allende Ca-Al-rich Inclusions <i>T. J. Fagan, G. J. MacPherson, and G. L. Kim</i>	5204
Chandra X-Ray Observations and the Spallogenic Origin of Shortlived Radionuclides <i>E. D. Feigelson, S. Wolk, and G. J. Consolmagno</i>	5109
Carbon, Nitrogen and Noble Gases in Diamond Separates from the Novo-Urei Ureilite <i>A. V. Fisenko, A. B. Verchovsky, L. F. Semjonova, and C. T. Pillinger</i>	5159
Element Hosts in Anhydrous IDPs: A Test of Nebula Condensation Models <i>G. J. Flynn, L. P. Keller, and S. R. Sutton</i>	5091

Discovery and Terrestrial Age of FRO 01149, an Extremely Small, Weathered and Old H-Chondrite Found on Top of Frontier Mountain, Antarctica <i>L. Folco, K. C. Welten, K. Nishiizumi, and D. J. Hillegonds</i>	5123
Elemental Fractionation and Mobilization in Equilibrated L Falls Due to Shock-related Heating <i>J. M. Friedrich and M. E. Lipschutz</i>	5047
Constraining the Early Solar System Cm/U Ratio <i>J. M. Friedrich and U. Ott</i>	5127
Chemical Classification of Asteroidal Material: Implications from Chondrite Chemical Diversity <i>J. M. Friedrich, A. Morlok, and S. F. Wolf</i>	5142
IDP Carbon and Mineral Phase Characterization by High Resolution Confocal Raman Imaging <i>M. Fries, L. Nittler, A. Steele, and J. Toporski</i>	5190
The Natural Remanent Magnetization and Magnetic Minerals of Tagish Lake (CI2) <i>M. Funaki, M. Zolensky, and N. Imae</i>	5057

3D TOMOGRAPHIC MEASUREMENTS ON ALLENDE VOLUMES – CONSTRAINTS ON THE FORMATION AND ACCRETION OF CHONDRULES AND MATRIX.

D. S. Ebel¹, T. W. Schoenbeck^{1,2}, and H. Palme². ¹American Museum of Natural History, Central Park West at 79th Street, New York, NY, 10024, ²University of Cologne, Institute for Mineralogy and Geochemistry, Zuelpicher Str 49b, D-50674 Koeln. E-mail: debel@amnh.org.

Introduction: Did chondrules and matrix material in carbonaceous chondrites form and accrete in closed, local chemical systems of solar composition [e.g.-2]; or where chondrules formed in one place, then transported to combine with matrix in some other region of the protoplanetary disk [e.g.-1]? This is a central issue in deducing the early history of the solar system.

Chondrules and matrix in some carbonaceous chondrites were shown by [2], using thin-section analysis, to be complementary in terms of their bulk chemical composition. Critical measurements include: (1) bulk chemical compositions of the meteorite and individual components; and (2) volume proportions of component chondrules, CAIs, dark inclusions and matrix. To address item (2), we used x-ray computer-aided microtomography (XR-CMT) to determine the exact volumetric proportions of chondrules and matrix in Allende (CV3). Despite its altered nature, Allende is well-suited for study because chondrules and matrix are chemically different and easy to distinguish in tomographic datasets.

Method: Tomographic images of two ~6x6x12mm equally sized Allende samples were collected using 40-42 KeV x-rays on the GEOCARS beamline of the Advanced Photon Source (APS) at Argonne National Laboratory in Illinois [3]. Image analysis programs were used to separate volume elements (voxels) within the images by their average x-ray attenuation. Repeated measurements of the whole section and smaller subsections showed that the resulting chondrule/matrix ratio can be determined with accuracy better than 5%. Chondrule and matrix compositions were also obtained by broad beam microprobe analysis of thin sections cut from the volumes.

Results: Both samples are expected to have the same bulk chemistry, and the matrix of both samples is found to be isochemical. However, the chondrule/matrix ratios differ by nearly a factor of two. Chondrule chemical compositions must, therefore, differ in the two samples.

Discussion: The close, complementary relationship between chondrule chemistry and matrix chemistry supports a highly localized, isochemical scenario for both the chondrule-forming and the chondrite accretion processes. Hypotheses [e.g.-1] which form chondrules in one region of the solar nebula, then mix them with matrix elsewhere, can be firmly excluded.

Acknowledgments: Use of the APS was supported by the U.S. Department of Energy, Office of Basic Energy Science under Contract No. W-31-109-ENG-38. T.S. was supported by the Annette-Kade Foundation at AMNH. The IDL program 'blob3d' was provided by R. Ketcham, U. Texas, Austin.

References: [1] Shu F.H. et al. (1997) *Science* 277, 1475-1479. [2] Klerner S. & Palme H. (2000) *MAPS* 35, Supp.A89. [3] Murray J. et al. (2003) LPSC XXXIV, Abs. #1999.

**I-XE AGE OF THE YAMATO 74191 (L3.6) CHONDRITE:
LATE CLOSURE TIME FOR I-XE SYSTEM WITH
ENRICHMENTS IN HALOGENS**

N. Ebisawa¹, R. Okazaki² and K. Nagao³. ^{1,3}Laboratory for Earthquake Chemistry, Graduate School of Science, University of Tokyo, Hongo, Bunkyo-ku, Tokyo 113-0033, Japan. E-mail: nagao@eqchem.s.u-tokyo.ac.jp: ²Department of Earth and Planetary Sciences, Faculty of Sciences, Kyushu University, Hakozaki, Fukuoka 812-8581, Japan.

Introduction: Yamato 74191 is classified as L3.6 chondrite. The meteorite is characterized by a very high concentration of neutron-produced ⁸⁰Kr and ⁸²Kr from Br and ¹²⁸Xe from ¹²⁷I along with high concentration of ¹²⁹Xe from extinct ¹²⁹I ($T_{1/2}=15.7$ Ma) [1]. The neutron-produced ¹²⁸Xe shows nice correlation with radiogenic ¹²⁹Xe excess with $[^{129}\text{Xe}]_r/[^{128}\text{Xe}]_n=263$. The $(^{80}\text{Kr}/^{82}\text{Kr})_n$ is about 2.6, which is very close to the estimated value from the resonance integrals of ⁷⁹Br and ⁸¹Br in the energy range of 30-300 eV [1,2]. Because cosmic-ray exposure age of 10 Ma [1] is in the range for most chondrites and fluence of cosmic-ray produced secondary neutron is in the order of 10^{15} n/cm² [2], the high concentrations of halogen-derived isotopes must indicate high concentration of halogens in this meteorite.

Experimental Method: We have reanalyzed noble gases for bulk samples and also measured noble gas micro-distribution using a laser heating technique to confirm the previously reported noble gas data. After that the meteorite was studied using a newly developed experimental apparatus for Ar-Ar and I-Xe dating of meteorites at the Radioisotope Center, University of Tokyo. An ion counting system has been installed to the VG3600 noble gas mass spectrometer. A new small extraction furnace and a laser microprobe enable us to measure noble gases from small samples irradiated by neutrons. Fragments of Yamato 74191 have been measured for I-Xe age. Bjurböle and Allende meteorites were also measured as reference samples.

Results and discussion: Obtained ¹²⁹Xe*/¹²⁸Xe* ratios in high temperature extraction steps are 0.68 and 2.23 for Y-74191 and Bjurböle, respectively. The ratio of 2.09 for Allende is similar to that for Bjurböle, indicating almost same formation ages for these meteorites. Contrary to the Allende meteorite, the value for Y-74191 indicates an I-Xe closure time of about 70 Ma later than that of Bjurböle. Very late closure times (>50Ma after Bjurböle) have been reported only for meteorites with high petrologic types (5 and 6) [3,4] Hence, the late closure time of I-Xe system is the first observation for the low petrologic type (L3.6) meteorite. The high concentrations of halogens in Y-74191 might have resulted by an aqueous alteration occurred on its parent body. Mechanism of halogens enrichments and their host phases will be investigated using techniques of SIMS, EPMA and laser microprobe noble gas extraction in the future work.

References: [1] Takaoka N. and Nagao K. 1980. *Z. Naturforsch.* 35a, 29-36. [2] Eugster O. et al. 1993. *Geochimica et Cosmochimica Acta* 57, 1115-1142. [3] Swindle T.D. 2002. *in* Noble Gases in Geochemistry and Cosmochemistry. *Rev. Mineralogy & Geochemistry*, Vol. 47. 101-124. [4] Brazzle R.H. et al. 1999. *Geochimica et Cosmochimica Acta* 63, 739-760.

CALCULATION AND PREDICTION OF HYDROTHERMAL ZONES AND IMPACT CONDITIONS ON ARGYRE PLANITIA, MARS.

J. C. Echaurren¹, A. C. Ocampo². ¹Codelco Chuquicamata, Chile, jecha001@codelco.cl, ²European Space Agency, ESTEC Keplerlaan 1, 2200 AG, Noordwijk, Netherlands, adriana.ocampo@esa.int

Synopsis: Argyre Planitia, named in 1973, is among one of the largest impact basins on Mars with a diameter of about 868 km, Argyre is located at S49.4 deg and W42.8 degrees. Argyre was part of a larger surface hydrological system (the Chese Trough Sanders, 1979) that also included two large valley networks draining the Margaritifer Sinus region northwest of Argyre. The morphometry of these systems suggest a combination of precipitation and groundwater sapping, with surface runoff for their formation (Grant and Parker 2002) [1], distributions of dust devil track has been studied on Argyre too [2]. This work is an application of mathematical models [3] for the determination of impact conditions, and for the prediction of possible hydrothermal zones generated after of the impact. All the calculations are obtained using a HP 49g, which is Scientific Programmable Graphing Calculator with 1.5 Mb in RAM memory.

Analytical Method and Results: According this model [3] the asteroid diameter is ~ 307.55 km, with a velocity and impact angle of ~ 14.69 km/s and $\sim 74.33^\circ$ respectively. The number of rings are calculated in ~ 294.11 with a crater profundity of ~ 5.40 km and melt volume of $\sim 3,185,768$ km³. The number of ejected fragments are estimated in $\sim 1.14E14$ with sizes of ~ 6.35 m. The total energy in the impact is calculated in $\sim 1.56E33$ Ergs, i.e., $\sim 37,085$ millions of Megatons. Before of the erosion effects the transient crater is estimated in ~ 581.85 km, the hydrothermal zone (hydrothermal systems) is of ~ 182.26 km to 290.93 km from the nucleus of impact. The lifetimes estimated are of ~ 47.74 Ma to 74.52 Ma with uncertainties of $\sim \pm 1.3133\%$ to $\pm 3.5391\%$, i.e., from ± 0.63 Ma to ± 1.96 Ma. Hydrothermal temperatures from 0.25 years to 1,400 years are estimated in $\sim 320^\circ\text{C}$ to 125.64°C (epithermal). The fragments are ejected to $\sim 4,605.66$ km from the impact center, with a velocity of ejection of ~ 4.79 km/s, ejection angle of $\sim 24.21^\circ$ and maximum height of ~ 517.79 km.

Conclusions: The numerical predictions for hydrothermal systems on Argyre, shows possible Kat thermal ($\sim 320^\circ\text{C}$) and Epithermal ($\sim 125.64^\circ\text{C}$) activity inside of the crater in the interval [182.26 km, 290.93 km]. Hydrothermal systems have long being proposed as good candidates for niches of life, the impact genesis of Argyre may have produced such environment conducive to life.

References: [1] Parker T. J., Grant J. A., Anderson F. S., and Banerdt W. B., (2003), Sixth International Conference on Mars, 3274.pdf. [2] Whelley P. L., Balme M. R., and Greeley R., (2003), Lunar and Planetary Science, 1769.pdf. [3] Echaurren J., and Ocampo A.C., (2003), EGS-AGU-EUG Joint Assembly.

NEW CALCULATIONS AND ESTIMATIONS FOR HYDROTHERMAL ZONES AND IMPACT CONDITIONS ON CHICXULUB, EARTH AND ISIDIS PLANITIA, MARS.

J. C. Echaurren¹ and A. C. Ocampo², ¹Codelco Chuquicamata, Chile, jecha001@codelco.cl, ²European Space Agency, ESTEC Keplerlaan 1, 2200 AG, Noordwijk, Netherlands, adriana.ocampo@esa.int

Synopsis: Chicxulub [1] is among the largest impact crater on Earth and a good analogue for Mars impact processes. Mars's Isidis Planitia [2] is one of the largest impact Planitias on Mars with a diameter of about 1,238 km. Isidis is located at N 14.1 deg and W 271.0 degrees and is the boundary between ancient highlands and the Northern Plains. The exceptionally well-preserved Chicxulub crater is located in the Peninsula of Yucatan in Mexico, and research has identified at least 3 concentric structural rings, which comprise a complex ~ 200 km diameter impact basin.

Analytical Method and Results: Our model [3,4] shows for Chicxulub that the asteroid diameter is ~ 7.01 km, with a velocity and impact angle of ~ 47.38 km/s and ~ 33.12° respectively. The number of rings are calculated in ~ 5.73 with a crater profundity of ~ 1.31 km and melt volume of ~ 37,414 km³. The number of ejected fragments are estimated in ~ 1,903 millions with sizes of ~ 5.66 m, the asteroid density is ~ 5.39 g/cm³. The total energy in the impact is calculated in ~ 1.2E30 Ergs, i.e., ~ 571 millions of Hiroshima. The hydrothermal zone is of ~ 61.2 km to 98 km from the nucleus of impact. The lifetimes estimated are of ~ 1.19 Ma to 1.86 Ma with uncertainties of ~ +/- 0.0076 Ma to +/- 0.0131 Ma. Hydrothermal temperatures for 0.25 years to 1,400 years are estimated in ~ 246.34°C to 96.65°C. The fragments are ejected to ~ 500.04 km from the impact center, with velocity of ejection of ~ 5.87 km/s, ejection angle of ~ 4.10° and maximum height of ~ 8.97 km.

For Isidis Planitia, the asteroid diameter is ~ 438.65 km, with a velocity and impact angle of ~ 19.42 km/s and ~ 74.09° respectively. The number of rings could be ~ 206 with a crater profundity of ~ 4.8 km and melt volume of ~ 5,765,600.6 km³. The number of ejected fragments are estimated in ~ 3.3E14 with sizes of ~ 6.35 m. The total energy in the impact is calculated in ~ 2.78E33 Ergs, i.e., ~ 66,110 millions of megatons. The hydrothermal zone is of ~ 69.69 km to 617.63 km from the nucleus of impact. The lifetimes estimated are of ~ 68.09 Ma to 106.28 Ma with uncertainties of ~ +/- 0.88 Ma to +/- 3.74 Ma. Hydrothermal temperatures for 0.25 years to 1,400 years are estimated in ~ 527.63°C to 207.16°C. Finally the fragments are ejected to ~ 79,276 km from the impact center, with velocity of ejection of ~ 24.42 km/s, ejection angle of ~ 75.18° and maximum height of ~ 74,894 km, these enormous distances could to eject the fragments out of the Mars planet, in a closed orbit.

All the calculations are obtained using a HP 49g, which is a Scientific Programmable Graphing Calculator with 1.5 Mb in RAM memory.

References: [1] Pope, K.O., Ocampo, A.C., Kinsland, G.L., and Smith, R. (1996) *Geology*, 24, 527-530. [2] Scott, D., and Tanaka, K. (1986) *Geological Survey Misc. Inv. Map*, I-1802-A. [3] Pope, K.O., Baines, K.H., Ocampo, A.C., and Ivanov, B.A. (1997) *Journal of Geophysical Research*, 102, 21,645-21,664. [4] Echaurren, J.C., and Ocampo, A.C. (2003) *EGS-AGU-EUG Joint Assembly*.

A MATHEMATIC MODEL FOR THE ARAGUAINHA IMPACT STRUCTURE, BRAZIL, SOUTH AMERICA. J. C. Echaurren¹, A. C. Ocampo² and M.C.L. Rocca³, ¹Codelco Chuquicamata, Chile, jecha001@codelco.cl, ²European Space Agency, ESTEC Keplerlaan 1, 2200 AG, Noordwijk, Netherlands, adriana.ocampo@esa.int, ³Mendoza 2779-16A, Ciudad de Buenos Aires, Argentina, (1428DKU), maxrocca@hotmail.com. This work was partially funded by The Planetary Society, CA, USA.

Synopsis: As 2004, the Araguainha impact structure (S 16°46' W 52°59') is South America's and Brazil's largest. Diameter: 40 km., Age: 246 Ma. Although it is eroded it still has the typical multi-ring shape configuration of large impact structures. Rocks exposed are Paleozoic sediments. The structure includes a 6 km central uplift of basement granite with heavily faulted and deformed rocks. Evidence for the origin of Araguainha in an impact event comes from breccia found near its center, shatter cones, shocked Quartz showing PDFs and melted rocks. Araguainha multi-ring shape is typical for impacts of its size [1, 2, 3]. The mathematical model is applied in quantum formalism, polynomial elements and Korteweg-DeVries (KDV) soliton theory [4], using a HP 49g, which is a Scientific Programmable Graphing Calculator with 1.5 Mb in RAM. For the impact event are used the following parameters: diameter ~ 40 km, circular shape, basement composition ~ granitic.

Analytical Method and Results: According this model the asteroid diameter is ~ 1.3 km, with a velocity and impact angle of ~ 21.71 km/s and ~ 88.74° respectively. The number of rings are calculated in ~ 1.41 with a crater profundity of ~ 2.7 km and melt volume of ~ 3,383 km³. The number of ejected fragments are estimated in ~ 64.24 millions with sizes of ~ 3.24 m, the asteroid density is ~ 5.46 g/cm³. The total energy in the impact is calculated in ~ 9.28E28 Ergs, i.e., ~ 44.18 millions of Hiroshimas (~2.21 millions of Megatones), and the pressures are ~ 22.33 Gpa. Before of the erosion effects the transient crater is estimated in ~ 26.83 km with an uplift of ~ 1.49 km, the hydrothermal zone (hydrothermal systems) is of ~ 6.37 km to 13.41 km from the nucleus of impact. The lifetimes estimated are of ~ 239,702 years to 356,910 years with uncertainties of ~ +/- 0.6545% to +/- 1.9195%, i.e., from +/- 1,569 years to +/- 4,601 years. Epythermal temperatures from 0.25 years to 1,400 years are estimated in ~ 191°C to 76°C (not epythermal). The fragments are ejected to ~ 238 km from the impact center, with a velocity of ejection of ~ 2.56 km/s, ejection angle of ~ 10.46° and maximum height of ~ 10.98 km. Finally the maximum density for the fragments is calculated in ~ 5.46 g/cm³, the minimum density is estimated in ~ 4.08 g/cm³, and the combined density for these fragments is calculated in ~ 2.34 g/cm³.

References: [1] Engelhardt W.V., Mathai S.K. and Walzbach J. (1992), *Meteoritics* 27: 442-457. [2] Crosta A.P. (1987), in *Research in Terrestrial Impact Structures*, J. Phol editor, pp.30-37, Vieweg and Sohn, Germany. [3] Hammerschmidt K. and vo Engelhardt W. (1995), *Meteoritics* 30: 227-233. [4] Echaurren J., and Ocampo A.C., (2003), EGS-AGU-EUG Joint Assembly.

WATER-SOLUBLE SALTS IN OMAN DESERT CHONDRITES.

D. Eggenschwiler¹, U. Krähenbühl¹ and B. Hofmann².

¹Department of Chemistry and Biochemistry, University of Bern, Freiestr. 3, 3012 Bern, Switzerland. ²Natural History Museum Bern, Bernastr. 1, 3005 Bern, Switzerland

Introduction: Cut surfaces of chondritic meteorites collected in the central deserts of Oman in 2001-2003 show often efflorescence of salts after storage under room conditions. Analyses by EDS showed a predominance of Mg, Fe and Cl. The role of this salt was studied in the alteration of the chemical composition of meteorites by weathering originating from the prolonged resting of these specimen in the deserts of Oman by measuring the water-extractable ion concentrations in three meteorites.

Experiments: Salts were observed on surfaces that were cut with polypropylene alcohol as coolant. Three L chondrites of similar size but from different localities were studied showing different degrees of weathering (W1, W2, W4) and having terrestrial ages of 5000 and 17000 years, respectively. A slice of 5 mm was cut out of the meteorites. Out of these slices rods were cut and the rods were divided into pieces (~5x5x10mm, 1g mass). Series of samples forming profiles from the surface to the interior of the meteorites were contacted with water (1:10 dilution) for 24 hours and the resulting solution measured for the ions of interest by ion chromatography (F, Cl, NO₃ and SO₄) and by ICP-OES (Na, Mg, K, Ca, Fe, Sr and Ba). The concentrations of water-extractable elements were measured in soil samples (<0.15 mm fraction) from the same desert areas to obtain background salt concentrations. For seven meteorite samples weight loss/gain upon drying at 100°C followed by storage under room conditions was studied.

Results: From the soluble ions Cl and Fe dominate the resulting solutions by more than an order of magnitude. We do not find a diffusion controlled uniform decrease of the soluble compounds from the surface to the interior of the meteorites as measured for halogens in Antarctic chondrites [1]. It seems that the presence and number of cracks and veins control the transport of contaminants into the interior of the meteorites. The presence of localized veins is also indicated by the fact that a second series of samples from the same meteorite shows rather different leaching results. Weathering mobilizes chlorine from soils and leads to its enrichment in meteorite, aiding the oxidation of native iron into the soluble FeCl₂ compound, which is concentrated along veins and cracks. The bulk iron concentration in desert soil is about half the one in the meteorite samples, leaching of soil samples only liberates very small quantities of Fe due to its oxidized state in the soil. Among the ions leached from the meteorite samples, iron originates from the meteorite while chlorine must be a contaminant from the desert. Drying at 100°C led to a weight loss of 0.23±0.07wt.% in seven samples. After 150 days of reequilibration under room conditions, 51-79% of the lost mass was regained, indicating the presence of a hygroscopic constituent.

Conclusions: Weathering of meteorites influencing their composition in hot deserts is controlled by temperature regime, humidity and local composition of the soil and the duration of all these processes. The degree of alteration is therefore rather unique for every single specimen. The strong enrichment of chlorine in some chondritic meteorites in the Oman desert and the hygroscopic nature of Fe and Mg chlorides indicate the presence of a chloride brine in the pore space.

References: [1] Langenauer M. and Krähenbühl U. 1993 *Earth and Planetary Science Letters* 120: 431-442

A SUPER-HARD, TRANSPARENT CARBON FORM, DIAMOND AND SECONDARY GRAPHITE IN THE HAVERÖ UREILITE: A-FINE-SCALE MICRORAMAN AND SYNCHROTRON TOMOGRAPHY.

A. El Goresy¹, Ph. Gillet², L. Dubrovinsky³, M. Chen⁴ and T. Nakamura⁵, ¹Max-Planck-Institut für Chemie, 55128 Mainz, Germany. E-mail: goresy@mpch-mainz.mpg.de, ²Ecole Normale Supérieure de Lyon, 69364 Lyon, France, ³Bayerisches Geoinstitut, Universität Bayreuth, 95440 Bayreuth, Germany, ⁴Guangzhou Institute of Geochemistry, CAS, 510640 Guangzhou, China, ⁵Dept. Earth and Planet. Sci., Fac. of Sci. Kyushu Univ., Hakozaki, Fukuoka 812-8581, Japan.

Introduction: The Haverö ureilite was subjected to a strong shock event that induced the inversion of the primary carbon phase to diamond [1,2]. Our microscopic inspection of polished sections revealed that the carbon islands contain different carbon polymorphs in a remarkable petrographic setting and depicting contrasting relief with consistent spatial arrangement: (a) low relief fine-grained opaque matrix of diamond and graphite, (b) very high-relief (up to 12 μm high) ragged transparent islands (< 40 μm in diameter) of carbon with heavily gouged surfaces, and (c) a > 30 μm layer of polycrystalline graphite separating the carbon islands from the surrounding olivine and pyroxene matrix.

Results: Laser microRaman investigations revealed that the low-relief lithology consists of diamond with the characteristic one-phonon band at 1331 cm^{-1} and secondary graphite depicting the characteristic G band at 1582 cm^{-1} . Evidently this lithology does not contain compressed graphite [3]. The spectra of the high-relief lithology depict the following bands: 336, 380, 468, 567, 750, 863, 1027, 1122, 1211, 1419, 1508, 1604, and 1700 cm^{-1} in addition to the characteristic Raman band of diamond at 1329 cm^{-1} and the “D” band of graphite at 1375 cm^{-1} [4]. The outer layer of polycrystalline graphite reveals a small Raman band of diamond at 1322 cm^{-1} , small graphite “D” and a sharp G band at 1364 cm^{-1} and 1572 cm^{-1} , respectively. This polycrystalline graphite is secondary formed by pervasive back transformation of diamond or relaxation of compressed graphite (or both) at high post-shock temperatures [5].

Discussion: The Haverö ureilite contains a super-hard carbon form that was not encountered naturally, produced in static or dynamic high-pressure experiments or predicted by theoretical calculations. Polishing hardness of this phase is superior to that of diamond. The petrographic setting is indicative of maximum densification in the inner most regions of the carbon islands. The outer most regions of the islands were subjected to high post-shock temperatures thus leading to pervasive back transformation of shock-induced diamond or recrystallization of compressed graphite to highly ordered polycrystalline graphite. Fine-scale synchrotron investigations of the super-hard form are in progress. The nature of the precursor carbon species, if graphite books, kerogenes, polycrystalline graphite or poorly graphitized carbon is unknown. Scrutinizing the nature of the precursor carbon will also be addressed by synchrotron microbeam tomography.

References: [1] Ramdohr P. 1972. *Meteoritics* 7, No. 4:565–571. [2] Neuvonen K. J. et al. 1972. *Meteoritics* 7, No. 4:515–531. [3] Nakamura Y. and Aoki Y. 2000. *Meteoritics & Planetary Science* 35:487-493. [4] Wopenka B. and Pasteris J. D. 1993. *American Mineralogist* 78: 533–557. [5] Nakamura T. et al. 2000. *Meteoritics & Planetary Science* 35:A117.

THE CHICXULUB IMPACT: RESULTS OF PETROPHYSICAL AND PALEOMAGNETIC INVESTIGATIONS

T. Elbra¹, L. J. Pesonen¹, T. Kenkmann², J. Smit³. ¹Laboratory for Solid Earth Geophysics, University of Helsinki. E-mail: tiu.elbra@helsinki.fi. ²Institute of Mineralogy, Museum of Natural History, Humboldt University of Berlin. ³Department of Sedimentology, Vrije University, Amsterdam.

The Chicxulub impact event and its relation to the global Cretaceous -Tertiary (K/T) mass extinction has recently resulted into new hot debates. Here we present petrophysical and paleomagnetic data of the CSDP Yaxcopoil YAX-1 drillcore to clarify dating aspects of the issue. Paleomagnetic measurements of the drillcore, coupled with petrophysical data provide a tool of isolating various units including the impact layer, the K/T boundary and the post-impact sequences. NRM and susceptibility values of samples from pre- and post-impact layers show that most samples are weakly magnetized (mainly dia- or paramagnetic with a possible weak ferrimagnetic signal), with densities of 2700 kg m^{-3} in case of pre-impact and 2200 kg m^{-3} in post-impact (Tertiary) samples. The interval from 790 m to 900 m is exceptional. It includes the K/T boundary layer, and consists mainly of suevites and melt breccias. This interval has stronger magnetizations and therefore can be easily recognized by susceptibility and NRM data. Densities from this interval vary within range of 1900 (near to K/T-boundary) to 2600 kg m^{-3} (lower part). This tendency can be partly due to porosity and/or lithological changes.

The K/T-boundary event took place within the magnetic chron 29R. Our data reveal that magnetostratigraphy of the impact layer is more complex. The average inclination of the reversely magnetized impact layer is -37° . However, it is contaminated by a normal polarity component with an average inclination of $+30^\circ$. We interpret this complex data as mixture of materials or magnetizations from the chrons 29R - 31N, which were redeposited shortly after impact. Hydrothermal remagnetizations may also contribute to the mixed magnetizations observed in this interval.

A 3D INVESTIGATION OF VALLES MARINERIS

B. E. Elliott and J. G. Spray. University of New Brunswick.
E-mail: bev.elliott@unb.ca. University of New Brunswick.

Introduction: Exploration in three dimensions can assist in the identification and characterization of important features in the Valles Marineris canyon system. The Fledermaus software package [1] permits the use of large data sets of high-resolution, such as data from the Mars Global Surveyor and Odyssey missions. The result is an analysis that is comprehensive and beneficial to Martian studies. Fledermaus can construct Digital Terrain Models (DTMs), drape imagery, perform data analysis and produce 3D flights (movies). We want to demonstrate how this 3D investigation can improve our understanding of the characteristics of features in Valles Marineris.

Method: Fledermaus is a visualization software capable of processing large data sets and providing interactive three-dimensional data exploration and analysis. DMAGIC [1] is an application of the software that can process and prepare data files for Fledermaus. The first step is to create a DTM in DMAGIC using MEGDR global topographic maps [2]. Georeferencing and surface shading are then applied to the DTM. The color map can be altered at any time to better represent the data set. Images can be draped over the DTM resulting in a more detailed analysis of the area. Images that can be draped include MOC [3] and THEMIS [4] data. The second step is to assemble the DTM, shading, georeferenced and draped image files as Fledermaus objects. The final result is a three-dimensional object that can be analyzed in Fledermaus (the main application of the software). Fledermaus is also capable of producing three-dimensional flights through various terrains. The third step is to produce various flight paths that can best reveal important aspects in areas of interest within Valles Marineris. These flights can be recorded and played back as movies, which allow the viewer to see the canyon system in detail and up-close.

Discussion: The purpose of this study is to investigate features of Valles Marineris using 3D exploration techniques. Various canyons in Valles Marineris contain layers (e.g. Hebes, Candor and Ophir Chasmata). By using 3D exploration, we can investigate these layers in detail without distortion of the high-resolution data used. The draping of MOC data will reveal the locations of significant features and the draping of THEMIS data will help identify mineral and rock types. This allows us to identify the composition of the various layered sequences within the canyons.

References: [1] Fledermaus Reference Manual, version 6.0. 1999-2004. Interactive Visualization Systems Inc. Unpublished, Fredericton, New Brunswick. [2] Smith, D., Neumann, G., Arvidson, R.E., Guinness, E.A. and Slavney, S. 2003. "Mars Global Surveyor Laser Altimeter Mission Experiment Gridded Data Record", NASA Planetary Data System, MGS-M-MOLA-5-MEGDR-L3-V1.0. [3] Malin, M.C. 2003. "MOC Standard Data Product Archive", NASA Planetary Data Systems, MGS-M-MOC-2-NA/WA-SDP-L0-V1.0. [4] Christensen, P.R., Gorelick, N., Mehall, G., Murray, K., Bender, K. and Cherednik, L. 2002. "Mars Odyssey Thermal Emission Imaging System Standard Data Record", NASA Planetary Data System, ODY-M_THM-2-IREDR-v1.0; ODY-M_THM-2-VISEDV-v1.0; ODY-M_THM-3-IRRDR-v1.0; ODY-M_THM-3-VISRDR-v1.0. [5] Smith, D., Neumann, G., Ford, P., Arvidson, R.E., Guinness, E.A. and Slavney, S. 1999. "Mars Global Surveyor Laser Altimeter Precision Experiment Data Record", NASA Planetary Data System, MGS-M-MOLA-3-PEDR-L1A-V1.0.

TRACE ELEMENT ABUNDANCES IN CHONDRULES FROM KNYAHINYA (L/LL5) AND OUZINA (R4)

A. Engler¹, G. Kurat² and P. J. Sylvester³. ¹Dept. Mineral. Petrol., University of Graz, Graz, Austria, almut_engler@hotmail.com
²Dept. Geolog. Sci., University of Vienna, Vienna, Austria. ³Dept. Earth Sci., Memorial University of Newfoundland, St. John's, Newfoundland, Canada.

Introduction and Analytical Methods: Previously we discussed the trace element geochemistry of non-porphyrific objects in unequilibrated ordinary chondrites (UOC) [1] as well as in some carbonaceous chondrites [2]. Here we present some bulk trace element analyses of non-porphyrific objects in the EOC Knyahinya and the R chondrite Ouzina. For trace element analysis we used a VG Plasma Quad II+S ICP-MS with a 266 nm Q-switched Nd-YAG laser following procedures of [3], except that we used a wide beam (~40 µm) for bulk sampling.

Results: Trace element (TE) abundances in individual objects in *Knyahinya* are all fractionated with respect to CI. Normalized REE abundances are between 0.1 and 2 x CI, all have a positive Eu anomaly and La < Lu, refractory TE (Nb, Ta, U, Th, Ca, Sc, Hf, Zr) > HREE and medium volatile elements (MVE) Sr, Ba, Mn, V and Cr are at 1 - 2 x CI (~ HREE). A few exceptions have very low REE contents (Sm ~ 0.1 x CI) with high Eu (~ 1 x CI) and low Ca, Sc, Hf and Zr abundances (between 0.6 and 1.2 x CI). One BO chondrule is exceptional because it contains a large apatite.

Ouzina objects also have fractionated normalized TE patterns with REE at 0.8 – 8 x CI, La < Lu but no or very small +/- Eu anomalies. Most refractory TE have abundances ~ HREEs (Nb, Ta, U, Th, Zr, Hf) and the MVE Sr, Ba, Mn, V and Cr have abundances < HREE and decrease with increasing volatility. Exception is OZ8, a BO chondrule with unfractionated refractory TE + Sr + Ba and fractionated MVE abundances. *Knyahinya* and *Ouzina* objects have strongly fractionated Rb/Cs ratios (up to 10 x CI) and are surprisingly rich in W (0.1 – 0.7 x CI in *Knyahinya* and 0.9 – 2 x CI in *Ouzina*) – despite their very low metal contents.

Discussion: In contrast to bulk trace element abundance patterns of fine-grained and BO objects from UOC and CC [1,2,4,5], which usually are relatively flat with or without some abundance anomalies, the patterns of objects in *Knyahinya* (EOC) and *Ouzina* (R4) indicate a more complicated genesis likely due to late stage equilibration processes [e.g., 6]. The depletion trend of LREE with respect to HREE and high-field-strength elements (HFSE) apparently documents varying degrees of elemental transport into an external REE sink [e.g., 7] and restricted mobility of most refractory TE. Apparently, REE are mobile, HFSE are not and therefore have high abundances in the objects. MVE (some are ol/px-compatible) tend to have equilibrated, unfractionated abundances in *Knyahinya* and only slightly fractionated ones in *Ouzina* objects. The fractionate Rb/Cs ratio implies low original VE contents and restricted mobility of the large Cs ion. Abundance pattern trends in objects of the two chondrites are broadly similar, which suggests a similar evolution history for objects of the EOC and the R4 chondrites. Lack of an Eu anomaly and the high abundance of W in *Ouzina* objects apparently reflect processing under fairly oxidizing conditions.

Acknowledgement: Supported by FWF, Austria (P14938).

References: [1] Engler et al. 2003a 34th LPSC, #1689. [2] Engler et al. 2003b *MAPS* 38:A86. [3] Jenner et al. 1993 *GCA* 57:5099-5103. [4] Grossman and Wasson 1983 *GCA* 47:759-771. [5] Kurat et al. 1985 16th LPSC, 471-472. [6] Kurat 1988 *Phil. Trans. R. Soc. Lond. A* 325:459-482. [7] Rambaldi et al. 1981 *EPSL* 56:107.

EVIDENCE FOR A TWO-LAYER STRUCTURE OF THE ACAPULCOITE/LODRANITE PARENT ASTEROID AND 5 MA CRE AGE OF 4 NEW ACAPULCOITES

O. Eugster and S. Lorenzetti, Physikalisches Institut, University of Bern, 3012 Bern, Switzerland. E-mail: eugster@phim.unibe.ch

Introduction: A group of meteorites with achondritic textures and chondritic element composition, the acapulcoites and the lodranites (A/L), appear to originate from a parent body that shows the mineralogical features of the S-class asteroids. These meteorites sample a lithologically diverse asteroid, which includes rocks that are broadly chondritic in chemical composition and samples of partial melts [1]. There is strong evidence that the A/L have a common parent body: they have identical O-isotopic composition [2] and their cosmic-ray exposure (CRE) ages are in a narrow range of 4-7 Ma [3]. Only one acapulcoite, TIL 99002, shows a CRE age of 14.8 Ma [4].

Results: In this work we determined the He, Ne, and Ar isotopic abundances in the four acapulcoites, DHO 125, DHO 290, DHO 312, and GRA 98028. CRE ages were calculated based on the concentrations of cosmogenic ^3He and ^{21}Ne and appropriate production rates [3]. The CRE ages of the four acapulcoites are 5-6 Ma, within the typical range of this type of meteorites.

Discussion: The evidences from mineralogical, chemical, and oxygen isotopic characteristics clearly show that the A/L come from the same parent body. Furthermore, the CRE ages indicate that almost all A/L were ejected by one or two break-up events 4-7 Ma ago. By analogy to the onion-shell structure of the H-chondrite parent body [5] we propose that the A/L parent asteroid also had a layered structure. We suggest that the acapulcoites, like the H3/4 chondrites, originate from the outer layer of the parent body as they are fine grained, the temperature was never high enough for silicate partial melting, the peak temperature was 950-1050°C, and the ^{39}Ar - ^{40}Ar ages are in the range of 4503-4556 Ma. The lodranites, like the H5/6 chondrites, represent the inner shells of their parent asteroid, are coarse grained, show silicate partial melting and were heated to ~1100-1250°C, and the only two ^{39}Ar - ^{40}Ar ages are at the later end of the range for the acapulcoite ages, 4519 Ma for EET 84302 [6] and 4490 Ma for Gibson [7].

Acknowledgements: Work supported by the Swiss NSF.

References: [1] McCoy T. J. et al. (2000) *Icarus* 148, 29. [2] Clayton R. N. et al. (1992) *Lunar Planet. Sci.* 23, 231. [3] Terribilini D. et al. (2000) *Meteorit. Planet. Sci.* 35, 1043. [4] Patzer A. et al. (2003) *Meteorit. Planet. Sci.* 38, 1485. [5] Tieloff M. et al. (2003) *Nature* 422, 502. [6] Mittlefehldt D. W. et al. (1996) *Geochim. Cosmochim. Acta* 60, 867. [7] McCoy T. J. et al. (1997) *Geochim. Cosmochim. Acta* 61, 623.

DECIPHERING MULTIPLE ALTERATION EVENTS IN ALLENDE Ca-Al-RICH INCLUSIONS.

T. J. Fagan, G. J. MacPherson and G. L. Kim. Dept. Mineral Sciences, Smithsonian Institution, Washington, DC 20560-0119. E-mail: fagan.tim@nmnh.si.edu

Introduction: It is well-known that Ca-Al-rich inclusions (CAIs) from the oxidized CV3 Allende have undergone more extensive alkali- and FeO-rich metasomatism than their counterparts in the reduced CV3s [1,2,3]. Allende CAIs also experienced a stage of recrystallization to secondary grossular and monticellite [4]. We have identified yet another form of secondary reprocessing in the Allende CAIs: inclusion trails in melilite crystals. It is not known if the inclusion trails, Ca-Mg-Al-silicate veins, and iron-alkali metasomatism formed at the same time or during independent events. In order to assess relationships between these types of alteration and implications for nebular and parent body evolution, we have initiated a comparative study of the different secondary mineral assemblages in Allende CAIs. Here, we present a preliminary report mineralogy and textures in 4 type B1 CAIs, 4 type B2s, one compact type A and six fluffy type A (FTA) inclusions.

Textural types of alteration: *Alkali- and FeO-rich metasomatism.* The alkali-FeO-rich zones are concentrated interior to Wark-Lovering rims in all CAI types. This type of alteration is manifested by the occurrence of grossular fringes along primary melilite, fine laths of anorthite, nepheline and sodalite, and FeO-bearing spinel.

Ca-Mg-Al-silicate veins. The veins occur along melilite grain boundaries, and are dominated by fine-grained (<5 μ m) grossular and monticellite. Where the veins merge with alkali-FeO-rich rims, the grossular has a similar composition in both settings.

Inclusion trails. Tiny ($\leq 1 \mu$ m) crystallites decorate irregular surfaces within melilite crystals, and apparently represent healed fractures. These surfaces typically are 100 to 200 μ m long, and occur with simple planar, curved planar, and anastomosing planar geometries. In most cases, the individual crystals are equant, but some trails have vermicular, branching inclusions that are elongate in the plane of the healed fracture. Multiple phases may be present, but so far only spinel has been positively identified. Some of the inclusion trails pinch out in the interior of a melilite crystal, but most of the trails have at least one end that terminates at a Ca-Mg-Al silicate vein.

Alteration events: Whereas the Ca-Mg-Al-silicate veins could have formed by closed-system breakdown of melilite+anorthite [4], the alkali-FeO-enriched rims require ingress of volatile components. This implies that the vein-forming and alkali-FeO metasomatic events may have been separated in time or place of formation. If the veins post-date the metasomatism, as suggested by the constant grossular compositions where the veins intersect metasomatized regions, then the veins may have formed in a parent body setting. If so, their paucity in reduced CV3 CAIs, like that of Ca-Fe-rich silicates [5], may be related to locally very low porosity on the parent body. The inclusion trails may be related to flow of fluid along fractures, but the nature of the fluid remains to be determined.

References: [1] Sylvester P. J. 1993. *Geochim. Cosmochim. Acta* 57: 3763-3784. [2] Krot A. N. et al. 1998. *Meteorit. Planet. Sci.* 33: 1065-1085. [3] Komatsu M. et al. 1998. *Meteorit. Planet. Sci.* 36: 629-641. [4] Hutcheon I. D. and Newton R. C. 1981. 12th Lunar Planet. Sci. Conf. pp. 491-493. [5] MacPherson G. J. and Krot A. N. 2002. *Meteorit. Planet. Sci.* 37: A91.

CHANDRA X-RAY OBSERVATIONS AND THE SPALLOGENIC ORIGIN OF SHORTLIVED RADIONUCLIDES.
 E. D. Feigelson¹, S. Wolk², and G. J. Consolmagno³. ¹Dept. of Astronomy & Astrophysics, Penn State U. edf@astro.psu.edu
²Chandra X-ray Center, SAO, and ³Specola Vaticana

Introduction: Material derived from the interstellar medium, or injected from a supernova remnant or AGB star, or made via spallation by relativistic baryons in the solar nebula, can all contribute isotopically anomalous material to the solar nebula. The local spallation of material by an energetic young Sun [1] is an attractive source of short-lived radionuclides (^{7,10}Be, ⁴¹Ca, ²⁶Al) inferred to have been present in various CAIs, gas-rich grains and chondrules [2]. *In situ* spallation requires MeV particle fluences $\sim 10^5$ times above levels of contemporary cosmic ray and solar energetic particle (SEP) fluences [3,4,5]; but X-ray observations of pre-main sequence (PMS) stars' flaring levels can give direct empirical constraints on the viability of the spallation model.

Data: The high sensitivity and resolution of the *Chandra X-ray Observatory* launched in 1999 permits detailed characterization of the magnetic flaring of 1 M_⊙ PMS analogs of the early Sun, especially in the Orion Nebula Cluster (ONC) where ~ 1000 stars with ages ~ 0.5 -2 Myr are concentrated in a single field. Results from other PMS populations are very similar. Two 12-hour exposures made in 1999 and 2000 show that the mean X-ray luminosity of a complete sample of 43 $0.7 < M < 1.4$ M_⊙ ONC stars is $\langle \log L_x \rangle = 30.3$ erg/s in the 0.5-8 keV band, $\sim 10^3$ above the average active Sun level today. Twenty-eight of these stars exhibited intraday variability. While it is difficult to distinguish individual flares from quiescent levels from these short exposures, we estimate that 1 flare with $29.0 < L_{x,peak} < 31.5$ erg/s with X-ray energies 10^{32} to $> 10^{36}$ ergs occurs every 1-2 days in PMS solar analogs. This is $10^{1.5}$ times stronger and $10^{2.5}$ times more frequent than seen in the contemporary Sun. The estimated enhancement in MeV proton fluences is 10 times above the X-ray fluence, or a total of 10^5 times above SEP levels. We also hope to present preliminary results from the *Chandra Orion Ultradeep Project* (COUP) based on a 10-day nearly-continuous exposure of the ONC made in January 2003, to derive impulsive flare precursors to the long-duration events and the frequency distribution of flare intensities and durations, improving particle fluence estimates.

Discussion: All young solar analogs exhibit huge elevations in magnetic flare levels, with estimated baryon fluences consistent with the requirements of a nebular spallogenic origin for several short-lived meteoritic isotopic anomalies. These are supported by radio continuum studies of enhanced gyrosynchrotron emission in PMS stars [6]. However, the location and geometry of the flaring magnetic fields is uncertain and additional model assumptions must be made to assure that the flare particles efficiently impact nebular solids to produce the observed distribution of isotopic anomalies [5].

References: [1] Feigelson E. D. and Consolmagno G. J. 1982. 13th Lunar & Planetary Science Conference, pp. 213-214; Feigelson E. D. 1982. *Icarus* 51:155-163; Feigelson E. D. et al. 2002. *Astrophysical Journal* 572:335-349; Feigelson E. D. and Montmerle T. 1999. *Annual Reviews of Astronomy and Astrophysics* 37:363-408. [2] Goswami J. N and Vanhala H. A. 2000. *Protostars and Planets IV*, 963. [3] Gounelle M. et al. 2001. *Astrophysical Journal* 548:1051-1070. [4] Goswami J. N. et al. 2001. *Astrophysical Journal* 549:1151-1159. [5] Lee T. et al. 1998. *Astrophysical Journal* 506:898-912. [7] Guedel M. 2003. *Annual Reviews of Astronomy and Astrophysics* 40:217-261.

CARBON, NITROGEN AND NOBLE GASES IN DIAMOND SEPARATES FROM THE NOVO-UREI UREILITE.

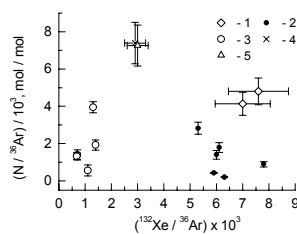
A. V. Fisenko¹, A. B. Verchovsky², L. F. Semjonova¹ and C.T. Pillinger². ¹Vernadsky Institute of Geochemistry and Analytical Chemistry RAS, Moscow, Russia, anatolii@fis.home.chg.ru. The Open University, Milton Keynes, UK.

The origin of diamond in ureilites is still debating. There are two the most popular explanations: (1) as a result of shock transformation from graphite caused by meteorite impact in the parent bodies [1-4], and (2) in a CVD process in the solar nebula [5-7].

We isolated a sample strongly enriched with diamond from the Novo-Urei ureilite and separated it into two density fractions in a heavy liquid at 2.9 g·cm⁻³. C, N, Ar and Xe have been analyzed simultaneously in the fractions by means of stepped combustion. Purity of the diamonds have been confirmed by Raman spectroscopy showing practical absence of graphite lines but surprisingly double peaks for diamond in the range of 1315-1335 cm⁻¹ that seems not to be observed in diamonds from other ureilites.

It has been found that concentration of N and noble gases in the less dense fraction (DNU-1) is ~1.5 times higher, than in the complimentary sediment (DNU-2). We believe the difference is due to the presence of aggregates with relatively low density made of smaller grains in DNU-1 compared to DNU-2 which consists mostly of single grains. Isotopic compositions of C (¹³C~-2‰), N (¹⁵N~-95‰) and noble gases as well as the elemental composition of the latter are similar in both fractions and to other diamonds analyzed before [8]. The obtained data together with published before, allow us to conclude that ureilite diamonds are likely formed as a result of shock transformation from graphite and amorphous carbon in the ureilites parent bodies. We also suggest that: (1) Carbonaceous material in the diamond-free ureilite ALH 78019 [9] seems to be contaminated with terrestrial atmospheric nitrogen during weathering since it is enriched with the nitrogen compared to other ureilites (Fig.). Therefore it does not show the light N signature normally observed in the ureilite diamonds. (2) The source of the light N in the ureilites might be presolar nanodiamonds (¹⁵N up to -350‰) that could be present in the carbonaceous material – precursor of the ureilites carbon.

Element ratios in ureilites. 1- present study; 2, 3 – carbon separates from Antarctic ureilites [10] for bulk (2) and magnetic fractions (3); 4, 5 – HF-HCl fractions of ALH 78019 [9] for total release (4) and without the first 300°C step (5).



References: [1] Lipschutz M.E. 1964. *Science* 143: 1431-1434. [2] Vdovykin G.P. 1970. *Meteoritika* 30: 95-103. [3] Nakamura Y., Aoki Y. 2000. *Meteorit. Planet. Sci.* 35: 487-493. [4] Valter A.A. et al. 2003. *Geochimica N10*: 1027-1035. [5] Matsuda J., Nagao K. 1989. *Geochim. Cosmochim. Acta* 53: 1117-1121. [6] Matsuda J. et al. 1991. *Geochim. Cosmochim. Acta* 55: 2011-2023. [7] Matsuda J., et al. 1995. *Geochim. Cosmochim. Acta* 59: 4939-4949. [8] Russell S.S. et al. 1993. *24th Lunar and Planet. Sci. Conf.* pp. 1221-1222. [9] Rai V.K., et al. 2002. *Meteorit. Planet. Sci.* 37: 1045-1055. [10] Yamamoto T. et al. 1998. *Meteorit. Planet. Sci.* 33: 857-870.

ELEMENT HOSTS IN ANHYDROUS IDPS: A TEST OF NEBULA CONDENSATION MODELS.

G. J. Flynn,¹ L. P. Keller² and S. R. Sutton³. ¹Dept. of Physics, SUNY-Plattsburgh, Plattsburgh NY 12901, USA. george.flynn@plattsburgh.edu. ²NASA Johnson Space Center, Houston, TX 77058. ³Dept of Geophysical Sciences and CARs, The University of Chicago, Chicago, IL 60637.

Introduction: Many anhydrous interplanetary dust particles (IDPs) are the most pristine samples of primitive Solar System dust that are currently available for laboratory analysis. Because these primitive, anhydrous IDPs show little or no evidence that they have experienced either thermal or aqueous alteration since their formation, they preserve materials that formed in the early Solar Nebula as well as presolar materials. Thus, we can test the applicability of equilibrium nebula condensation models to our Solar System by comparing the host mineral of each element with the host that is predicted by the nebula condensation models.

Samples: We have mapped the spatial distribution of most of the elements from K to Zn in ultramicrotome sections, each ~100 nm thick, in 3 primitive, anhydrous IDPs – L2011*B2, L2010B10, and L2009*F3, all of which are fragments of cluster IDPs. We employed a zone plate focused X-Ray Microprobe (XRM) at Sector 2 of the Advanced Photon Source (APS) at the Argonne National Laboratory to perform the element mapping. This XRM has ~150 nm spatial resolution, which is sufficient to resolve individual mineral grains in most of the anhydrous IDPs.

Results: Each element that we mapped was found to be localized within each IDP, with some element hot-spots being sub-micron in size.

K Results. L2011*B2 is a cluster fragment that contains a relatively high K concentration. The K is spatially correlated with the silicate in this particle. Nebula condensation models indicate that K should condense at ~1000 K into K-feldspar [1, 2]. However, Transmission Electron Microscope (TEM) examination of other ultramicrotome sections of this fragment indicate that the silicate in L2011*B2 is pyroxene, rather than feldspar.

S Results. Small S hot-spots were detected in each IDP. Most of the S is concentrated in Fe-sulfides, consistent with the prediction of nebula condensation models that S should condense at ~650 K into Fe-sulfide [1, 2].

Zn Results. The Zn is concentrated into small hot spots, which are collocated with S. This is consistent with the prediction of nebula condensation models that Zn should condense at ~660 K into Zn-sulfide [1, 2].

Cu Results: The Cu is concentrated into small hot spots, which are collocated with S. The equilibrium nebula condensation models predict that Cu should initially condense at ~1040 K into a metal alloy [1, 2].

Ca, Ti, Cr, Mn, and Ni Results. We also observed hot-spots of Ca, Ti, Cr, Mn, and Ni in the element maps. The host minerals of each of these elements will be determined by TEM, and compared to the predictions of the equilibrium nebula condensation models.

References: [1] Grossman, L. 1972, *Geochimica et Cosmochimica Acta*, **36**, 597-619. [2] Grossman, L. and Larimer, J. W. 1974, *Reviews of Geophysics and Space Physics*, **12**, 71-101.

DISCOVERY AND TERRESTRIAL AGE OF FRO 01149, AN EXTREMELY SMALL, WEATHERED AND OLD H-CHONDRITE FOUND ON TOP OF FRONTIER MOUNTAIN, ANTARCTICA. L. Folco^{1*}, K. C. Welten^{2*}, K. Nishizumi² and D. J. Hillegonds³. ¹Museo Nazionale dell'Antartide, 53100 Siena, Italy (e-mail: folco@unisi.it) ²Space Sciences Laboratory, University of California, Berkeley, CA 94720, USA, (*e-mail: kcwelten@uclink4.berkeley.edu); ³CAMS, Lawrence Livermore National Laboratory, Livermore, CA 94550, USA.

Introduction: In December 2001, a small (1.5 g) chondrite was found on top of Frontier Mountain (northern Victoria Land) by a PNRA team during a geomorphological survey. The meteorite was sitting on glacially eroded bedrock surfaces at an altitude of 2775 m (i.e., ~600 m above present day ice level), recording a past, yet undated, ice sheet overriding of Frontier Mountain. The meteorite, named Frontier Mountain (FRO) 01149, was classified as an H4 chondrite [1], and shows almost complete oxidation of the metal and sulfides, corresponding to weathering degree W4 on the scale of Wlotzka [2]. A second search effort on top of FRO in 2003 did not yield additional specimens.

Analytical Methods and Results: Due to the high degree of oxidation, an attempt to separate clean metal from ~1 g of this meteorite was unsuccessful. We thus dissolved ~95 mg of the bulk sample for measurements of cosmogenic ¹⁰Be, ²⁶Al, ³⁶Cl and ⁴¹Ca. In addition, we separated a grain-size fraction of >250 μm and leached this fraction with dilute HCl to remove weathering products and obtain clean silicate grains. We dissolved ~31 mg of this fraction for measurements of cosmogenic ¹⁰Be and ²⁶Al. Concentrations of ¹⁰Be, ²⁶Al, ³⁶Cl and ⁴¹Ca were measured by accelerator mass spectrometry at the CAMS facility at LLNL.

For ⁴¹Ca in the bulk sample, we only obtained an upper limit of <0.4 dpm/kg. Since most (if not all) of the metal and troilite in this meteorite was converted to Fe-hydroxides, we assume that the measured value represents ⁴¹Ca produced from Fe and Ca in the silicates, whereas ⁴¹Ca produced in metal and troilite was lost upon oxidation [3]. This upper limit of 0.4 dpm/kg thus corresponds to <2.4 dpm/kg(Fe+5*Ca). Based on a saturation value of 24 dpm/kg, this value indicates a terrestrial age >300 kyr. The ¹⁰Be concentrations of 7.3±0.1 dpm/kg corresponds to a terrestrial age of 1.6-2.2 Myr if we assume a ¹⁰Be production rate of 15-20 dpm/kg and an exposure age long enough (>5 Myr) to saturate ¹⁰Be. Measurements of ²⁶Al and ³⁶Cl (in progress) are necessary to further constrain the terrestrial age and exposure history of FRO 01149.

Conclusions. If the terrestrial age of ~2 Myr is confirmed by additional radionuclide measurements, FRO 01149 will be the third chondrite from Antarctica with such a high terrestrial age [4,5]. The difference is that the first two, Allan Hills (ALH) 88019 and Lewis Cliff (LEW) 86360 were found on the ice surface and were relatively fresh compared to FRO 01149. The relative freshness of the two old ALH and LEW meteorites led to the conclusion that these two meteorites spent most of their terrestrial residence time traveling within the ice. However, the high degree of weathering and the find location strongly suggest that FRO 01149 fell where it was found and spent most of its terrestrial residence time exposed on bedrock. The terrestrial age of FRO 01149 can thus constrain the last glacial overriding of Frontier Mountain and provide information on the glacial history of northern Victoria Land.

References: [1] Russell S. et al. (2002) MAPS 37, A157-A182. [2] Wlotzka F. (1993) Meteoritics 28, 460. [3] Welten K. et al. (2004) MAPS 39, 481-498. [4] Scherer P. et al. (1997) MAPS 32, 769-773. [5] Welten K. et al. (1997) MAPS 32, 775-780.

ELEMENTAL FRACTIONATION AND MOBILIZATION IN EQUILIBRATED L FALLS DUE TO SHOCK-RELATED HEATING.

J. M. Friedrich¹ and M. E. Lipschutz². ¹Max-Planck-Institut für Chemie, Department of Cosmochemistry, Joh.-J.-Becher-Weg 27, D-55128 Mainz, Germany. E-mail: fried@mpch-mainz.mpg.de. ²Purdue University, Department of Chemistry, 560 Oval Drive, West Lafayette, Indiana 47907-2084 USA.

Introduction: Of all major chondrite groups, L chondrites experienced the most extreme episode(s) of post-metamorphic shock-related alteration, culminating in the massive impact(s) disrupting the L parent(s) ~500 Ma ago. Our previous work indicated that shock-related (re)heating is the primary source of equilibrated L fall trace element compositional patterns; we found no relation between petrographic type and composition [1,2]. Our studies suggest differences arise from open-system loss of thermally labile elements along with subtle metal/silicate partitioning during the extended cooling of shock-heated bodies [1].

Methods: To further examine the role of open-system (re)heating on the compositional patterns of L chondrite falls, we compare the thermally labile element content of our large (n=48), chemically representative [3], L chondrite suite with those of artificially heated Krymka (LL3.1) [4].

Additionally, using the multivariate statistical metrics discriminant analysis (DA) and logistic regression (LR), we compare major element content of mildly- (n=12) and strongly- (n=25) shocked L chondrite suites. We chose this sub-suite because our trace element determinations were done on homogenized aliquots used for major elements quantification [cf. 1,5], making direct comparison with previous results unambiguous.

Results and Implications:

Trace elements and mobilization. When comparing volatile element content of our L suite with heated Krymka, several points become evident. First, mobile elements In, Bi, Tl are more markedly depleted in many strongly-shocked L chondrites than in 1000°-heated Krymka. Although Zn, Se, Te also show systematic depletions in highly-shocked L samples, only one sample shows depletion of these elements greater than Krymka heated to 650°. Zn, Se, and Te were likely partially retained in a S-rich partial melt that was incompletely segregated from bulk L material unlike In, Bi, and Tl, which were more readily vaporized during the same heating episodes.

Statistical comparison of major element content. Comparisons of our two L suites based on major lithophiles (SiO₂, MgO, Al₂O₃, CaO, Cr₂O₅) and permutations of them yield DA and LR model-dependent [1 and references therein] p-values of <0.05 (highly statistically significant). DA and LR comparisons based on major siderophile (and S) content (FeO, FeS, Fe_m, Ni) yielded poor separations with p-values >0.3. Excellent separation is possible when diverse geochemical species (e.g. MgO, Cr₂O₅, MnO, FeS; model-dependent p-values DA: 0.010 and LR: 0.008) are considered. Further investigation shows that, like trace elements, the strongly-shocked suite is enriched in lithophiles compared to mildly-shocked L falls with a corresponding mean depletion of siderophile content.

References: [1] Friedrich J. M. et al. 2004 *Geochim. Cosmochim. Acta*, in press. [2] Friedrich J. M. and Lipschutz M. E. 2002 Abstract #1086, 33rd LPSC. [3] Friedrich J. M. et al. 2003 *Geochim. Cosmochim. Acta* 67: 2467-2479. [4] Ikramuddin M. et al. 1977 *Geochim. Cosmochim. Acta* 41: 393-401. [5] Jarosewich E. 1990 *Meteoritics* 25: 323-337.

CONSTRAINING THE EARLY SOLAR SYSTEM Cm/U RATIO.

J. M. Friedrich and U. Ott. Max-Planck-Institut für Chemie, Department of Cosmochemistry, Joh.-J.-Becher-Weg 27, D-55128 Mainz, Germany. E-mail: fried@mpch-mainz.mpg.de.

Introduction: The relative abundances of r-process nuclides within early solar system material reflect the complexity of the r-process. For example, derived solar r-process residuals [1] show ^{182}Hf abundance is consistent with continuous r-process nucleosynthesis up to ~ 20 Ma before incorporation into the early solar system. However, using the same residuals, ^{129}I abundance would require a decay time of ~ 80 Ma. To accommodate this discrepancy, [2] suggested two types of r-processes that operate with different frequencies at different nuclidic mass ranges, each being main sources for either ^{129}I or ^{182}Hf . However, [3] favor co-production of these nuclides in a single process: they note the current $^{247}\text{Cm}/^{235}\text{U}$ limit of $<4 \cdot 10^{-3}$ [4] is incompatible with measured ^{182}Hf abundance because all recognized theories demand co-production of actinides with Hf-mass range nuclides. We have been performing measurements to improve estimates of the early solar system $^{247}\text{Cm}/^{235}\text{U}$ abundance ratio to address if a distinct nucleosynthetic process is necessary to account for the (high) early solar system ^{182}Hf abundance.

Table 1: Comparison of time between steady state and early solar system abundance ratios for selected short-lived radionuclides.

	^{129}I	^{182}Hf	^{244}Pu	^{247}Cm
$T_{1/2}$ (Ma)	16	9	81	15.6
Ref. Nuclide	^{127}I	^{180}Hf	^{238}U	^{235}U
Prod. Ratio [1,5,6]	1.4	1.4	0.7	0.53
Steady State ISM Ratio [†]	0.0032	0.0018	0.013	0.012
Early Solar System Abundance Ratio [4,5]	$1 \cdot 10^{-4}$	$1 \cdot 10^{-4}$	$7 \cdot 10^{-3}$	$<4 \cdot 10^{-3}$
$\Delta T_{\text{Steady State} - \text{ESS Abundance}}$	80 Ma	24 Ma	80 Ma	> 25 Ma

[†] Calculated using methods of [5] and references therein.

Methods: ^{247}Cm decays to ^{235}U through four nuclides with a half live of about 15.6 Ma. Deviations in $^{238}\text{U}/^{235}\text{U}$ ratios would likely be due to the former presence of ^{247}Cm . We have used high-precision mass spectrometric methods to investigate the U isotopic composition of a wide variety of early solar system components and sequential acid digestions of them [7]. For this work, in addition to new isotopic results, we quantified REE in isotopically analyzed sample aliquots to estimate the degree of actinide fractionation possible within each sample.

Results and Discussion: Aside from a refractory Allende residue showing an enticing +4‰ anomaly – which needs to be analytically verified – we have found no statistically significant deviations ($> \pm 1.8\%$) from the $^{238}\text{U}/^{235}\text{U}$ solar system value of 137.88 in any of the 22 CAI, chondrite, or eucrite samples investigated. Currently, we are pursuing additional measurements of separated early solar system components to investigate possible trends emerging between LREE/U ratios and $\delta^{235}\text{U}$. With our measurements, we will be able to shed new experimental light on nucleosynthetic theories.

References: [1] Arlandini C. et al. 1999 *Astrophys. J.* 525: 886-900. [2] Qian Y.-Z. et al. 1998 *Astrophys. J.* 494: 285-296. [3] Pfeiffer B. et al. 2001 *Nuc. Phys. A* 688: 575c-577c. [4] Chen J. H. and Wasserburg G. J. 1981 *Earth Planet Sci. Lett.* 52: 1-15. [5] Meyer B. S. and Clayton D. D. 2000 *Space Sci. Rev.* 92: 133-152 [6] Lingenfelter R. E. et al. 2003 *Astrophys. J.*, 591: 228-237. [7] Friedrich J. M. et al. 2004 Abstract #1575, 35th LPSC.

CHEMICAL CLASSIFICATION OF ASTEROIDAL MATERIAL: IMPLICATIONS FROM CHONDRITE CHEMICAL DIVERSITY.

J. M. Friedrich¹, A. Morlok², and S. F. Wolf³. ¹Max-Planck-Institut für Chemie, Department of Cosmochemistry, Joh.-J.-Becher-Weg 27, D-55128 Mainz, Germany. E-mail: fried@mpch-mainz.mpg.de. ²The Natural History Museum, Department of Mineralogy, Cromwell Road, London, SW7 5BD, UK. ³Indiana State University, Department of Chemistry, Terre Haute, IN 47809 USA.

Introduction: In summer 2005, the Hayabusa (MUSES-C) robotic explorer is due to arrive at asteroid 25143 Itokawa (1998 SF36) for extended observations and samples are due to be returned in summer 2007 [1]. These invaluable samples will be used to establish a concrete physical connection between the ordinary chondrites, their generally accepted S-class asteroid source [3] and the evolutionary processes affecting both. Individual Hayabusa researchers will likely have access to only small amounts (<< 100 mg) of material sampled from the outermost surface of 600m – 300m Itokawa rather than more representative (interior) material [1]. To investigate the effect of (surface) sampling and chondrite heterogeneity on the classification of and conclusions drawn from returned asteroidal material, we have compared several suites of H chondrites and H chondrite-derived material.

Methods: We used compiled H chondrite data from [4]. This includes 470 H chondrite chemical analyses including Mg (for normalization). We divided these into collections of likely surface material (solar gas rich, regolith breccias, chondrites with surface-process derived light/dark structures, and combinations of the above) and less processed “normal” material. Data used for statistical comparisons of differently processed H material was in some cases limited to that produced by [5] to eliminate possible analytical bias.

Results and Discussion:

Comparisons using common classification metrics. Major element comparison of our H chondrite suites show that the surface suite is slightly (>3%) enriched in Mg, Ca, Cr, Co, Ni and slightly (>2%) depleted in K and Mn. Other major elements are nearly identical. These differences are likely the result of brecciation processes. When comparing the same suites using common elemental classification ratios, (e.g. Mg/Si vs. Fe/Si) occasional separate compositional domains emerge, but overlap is either complete or total: as might be guessed, chemical classification should be possible using ratio-type classification metrics.

Statistical comparisons. We initially compare the major element composition of equilibrated and unequilibrated H chondrites to examine the univariate statistical significance of H chondrite chemical ranges. In this case, significant (>95% CL) differences emerge in C, Cr₂O₃, H₂O^{+/-}, Fe_{metal}, Fe_{total}, Ni. Similar significant differences (CaO replaces Cr₂O₃) exist with comparisons of Si normalized major elements. These differences seem likely due to metamorphic redox conditions and Fe_{total} content.

Our work is beginning to establish the diversity of material recognized as H chondrites. Additional methodical comparisons of H chondrites and other chemical groups will clarify sampling issues associated with asteroid sample return.

References: [1] Fujuwara A. et al. 2004 Abstract #1521, 35th Lunar and Planetary Science Conference. [3] Gaffey M. J. et al. 1993 *Meteoritics* 28: 161-187. [4] Koblitz J. 2003 METBASE ver. 6.0 CDROM. [5] Jarosewich E. 1990 *Meteoritics* 25: 323-337.

IDP CARBON AND MINERAL PHASE CHARACTERIZATION BY HIGH RESOLUTION CONFOCAL RAMAN IMAGING.

M. Fries¹, L. Nittler², A. Steele¹ and J. Toporski¹. ¹Geophysical Laboratory and ²Department of Terrestrial Magnetism, Carnegie Institution of Washington, Washington, D.C. 20015 E-mail: m.fries@gl.ciw.edu.

Interplanetary dust particles (IDPs) are typically several microns in diameter and contain carbon and other materials bearing structure on a sub-micron scale. Confocal Raman imagery with a spatial resolution of ~250nm is used here to probe for phase identification and characterization at the small scale necessary to resolve IDP internal structure [1]. IDPs L2036v4, L2036v5, and L2036v8 have been mounted on gold foil, pressed to minimize beam scattering effects and to reveal interior structure, and imaged using a WITec CRM 200 Raman imager. A 543 nm excitation laser was used generating 10 mW power at 0.1 s per pixel scan speed. Data collected includes planar imaging and depth profiling collected through linear scans with incremental focal length adjustment.

The collected data is dominated by carbon matrix material due to masking of other phases by optically absorptive carbon [2]. Depth profile Raman measurements reveal the presence of mineral grains within the carbon matrix, and some mineral grains are exposed by the pressing technique. Graphite crystallite size is calculated using Tuinstra's method [3-6] of carbon band intensity ratio measurement, yielding a distribution of particle sizes and spatial mapping of the graphite component of the system. Spectral matching is used to identify other phases, such as metal oxides and nitrides. This data will be presented, as well as comparison between topographic imagery as collected by SEM and phase distribution as measured by Raman imagery.

- [1] Fries, M. et al 2004. Abstract #2139. 35th Lunar & Planetary Science Conference [2] Wopenka, B. *EPSL* 88:221-231 [3] Tuinstra, F. and Koenig, J. 1970. *J. Chem. Phys.* 53:1126-1130 [4] Knight, D. and White, W. 1989. *J. Mater. Res.* 4:385-393 [5] Ferrari, A. and Robertson, J. 2000. *Phys. Rev. B* 61:14095-14107 [6] Matthews M. et al 1999. *Phys. Rev. B* 59:R6585-R6588

THE NATURAL REMANENT MAGNETIZATION AND MAGNETIC MINERALS OF TAGISH LAKE (CI2).

M. Funaki¹, M. Zolensky² and N. Imae¹. ¹National Institute of Polar Research, Tokyo; funaki@nipr.ac.jp, ²Johnson Space Center, NASA.

Introduction: Tagish Lake (CI2) is the most primitive among any known meteorites [1], [2]. Magnetite and pyrrhotite are very abundant, but pentlandite is minor. The hysteresis (J_s - H) and low temperature magnetic studies [3] yielded magnetite of mostly multi-domain. We studied natural remanent magnetization (NRM) of Tagish Lake and its carrier minerals based on the basic magnetic properties and microscopic observations.

NRM: Four samples with an orientation were obtained from the interior. Their NRMs were AF demagnetized to 100 mT, and were relatively stable up to 30mT. The directions made a cluster when they were demagnetized to 25 mT. A piece of sample was demagnetized thermally from room temperature to 630°C in the vacuum to 10^{-3} Pa. The intensity decayed gradually up to 530°C and then it increased, while the direction was not drastically changed to 630°C.

Thermomagnetic (J_s - T) and J_s - H curves: J_s - T curve of was obtained under the steady magnetic field 1.0 T. The sample showed irreversible curve with clearly defined Curie point at 610°C and minor ones at 340° and 510°C in the heating curve and 610°C in the cooling curve. Although the Curie point at 610°C is much higher than that of magnetite, it may overprint to magnetite and the other minerals with high Curie point (taenite or awaruite). Temperature dependence of coercive force (H_c) was stepwise decreased at 130°, 330° and 580°C, suggesting more complicate magnetic mineral assemblage as pyrrhotite, pentlandite and magnetite.

Microscopic observation: Iron sulfide grains and aggregate of fine-grained sulfide were confirmed around chondrule and clast, but larger magnetite were not recognized. In the state of NRM, no obvious clusters of magnetotactic bacteria appeared, while small and weak clusters were confirmed on some sulfide grains and some area on the matrix. When the sample was artificially magnetized, the strong clusters appeared on phyllosilicate around rims of clasts and chondrules.

Discussion: The magnetic mineral has been reported as magnetite of mostly multi-domain with $H_c=25$ -28 mT in Tagish Lake [3], inferring unstable NRM. However, our data indicated the relatively stable NRM up to 25 mT of the AF demagnetization and up to 630°C of the thermal demagnetization. The H_c values are large enough in comparison with paleomagnetic samples of the terrestrial rocks. From the viewpoints, the NRM of Tagish Lake seems to be significant. The magnetic minerals may consist of magnetite, pyrrhotite, pentlandite etc. to the contrary of the estimation by [3]. Distribution of these minerals on phyllosilicate suggests that the magnetic minerals were formed by hydrothermal alterations in the parent body. We concluded that the magnetic field existed in the Tagish Lake parent body during the hydrothermal alteration.

References: [1] Hiroi et al. (2001), *Science* 293, 2234-2235. [2] Zolensky et al. (2002), *Meteorite & Planetary Science* 37, 737-761. [3] Thorpe, et al. (2002), *Meteorite & Planetary Science* 37, 763-771